Published in : Physical Review E (2025), vol. 112, n°4, L043403
DOI: 10.1103/pznx-lrxq
Status : Postprint (Author's version)

BUCKLING AND ZIPPING OF A MAGNETIC RING UNDER GRAVITY

Adrien Wafflard*, Simon Van der Heyde, Jérémy Dhyon, Eric Opsomer et Nicolas Vandewalle

GRASP, Institute of Physics B5a, University of Liège, B4000 Liège, Belgium
**Contact author: adrien.wafflard@uliege.be*

KEYWORDS : Buckling ; Dipolar interaction ; Elastic deformation ; Granular materials ; Ab initio molecular dynamics ; Simulated annealing

ABSTRACT

Assemblies of magnetic beads, also called magnetostructures, exhibit interesting mechanical properties, adapting orientations of the dipoles to minimize the dipolar energy. A ring made of N spherical magnetic beads behaves like an elastic annulus. This elastic-like property is due to the dipolar nature of the particles. When submitted to gravity and as a function of its size, the initial circular shape of a magnetic ring is seen to experience flattening. This capsule-like shape appears when the number N of magnets reaches a critical point scaling with the Bond number $N_f \propto \mathrm{Bo}^{-1/3}$. When the number of magnets increases more and more, the ring starts to buckle and a flat object appears at a second critical point $N_z \propto \mathrm{Bo}^{-1} + b$. There, a zipping state corresponding to the attraction of two opposite sides is formed. We propose a theoretical approach to capture these scaling laws in agreement with experimental data. All shapes are also numerically obtained in a discrete element model confirming our findings.

Article Text

Soft matter systems inspired by living organisms often display rich mechanical behaviors, including deformation, locomotion, and shape transformation. In particular, elastic objects may exhibit fundamental instabilities such as buckling, a mechanical response to compression characterized by the formation of folds or wrinkles [1], and zipping, an adhesion-driven process where surfaces progressively bind or rebind due to gradients in adhesive energy [2,3]. These phenomena, resulting from the interplay between geometry, elasticity, and interfacial forces, are fundamental to numerous biological and synthetic systems.

Although buckling and zipping have been extensively studied independently, relatively few systems exhibit these behaviors in a coupled and tunable manner. Notable exceptions include biological tissues undergoing morphogenesis [4,5], elastocapillary assemblies [6], and specific magnetomechanical microsystems, in which buckling facilitates controlled deformation while zipping ensures surface contact or closure [7,8].

Recently, magnetic soft matter has emerged as a versatile platform for designing active and reconfigurable structures across multiple length scales. Magnetic colloids, for instance, self-

Published in : Physical Review E (2025), vol. 112, n°4, L043403
DOI: 10.1103/pznx-lrxq
Status : Postprint (Author's version)

assemble into dynamic structures capable of periodic deformation, functioning analogously to motors or machines [9–13]. Mesoscopic magnetoelastic systems exhibit large deformations, including buckling, folding, and shape reconfiguration, when subjected to external magnetic or mechanical stimuli [14–17]. These systems uniquely combine elastic responses with adhesive-like interactions mediated by dipoledipole forces.

Among magnetic soft systems, magnetostructures composed of permanent magnets have attracted significant attention due to their rich physical properties [18]. For instance, spherical magnets can self-assemble into diverse configurations such as chains [19,20], rings [18,21], tubes [22,23], disordered gels [24,25], and lattices [26]. When subjected to external fields, including gravity, fundamental questions regarding the structural stability and mechanical response of these assemblies arise [20,27].

In this Letter, we investigate a macroscopic magnetomechanical system composed of N dipolar magnetic particles arranged in deformable rings subjected to gravitational forces. By closing the ends of magnetic particle chains, we form rings capable of exhibiting complex mechanical responses, including flattening, buckling, and adhesion reminiscent of zipping. This system provides an insightful model for exploring how magnetic interactions and mechanical constraints combine to yield sophisticated shape transformations, with potential implications for reconfigurable materials and soft robotics.

Our dipolar spherical particles are made of an Nd-Fe-B alloy, known as strong permanent magnets. Three kinds of beads are considered, labeled $\mu_{\mathrm{Ni},5}$, $\mu_{\mathrm{Cr},5}$, and $\mu_{\mathrm{Cr},3}$, depending on their diameter d and coating. Their properties are referenced in Table I. We assume that each bead is a uniformly magnetized sphere.

Table I. Physical properties of the three types of beads used in our experiment.

	Diameter (mm)	**Mass (g)**	**Magnetization (Am2)**
μNi,5	5	0.5	6.25 ×10−2
μCr,5	5	0.5	6.77 ×10−2
μCr,3	3	0.1	1.46 ×10−2

Our experimental setup, sketched in Fig. 1, consists ofn two polymethylacrylate (PMMA) plates, separated by a distance slightly larger than the diameter d of the beads, to keep the system two-dimensional. To avoid inertial effects, those plates are initially horizontal ($\vartheta = 0^{\circ}$), and can rotate around an axis that is parallel to the plates. This allows us to increase ϑ, thus increasing gravity's component $g \sin \vartheta$ parallel to the ring's plan. A camera is fixed to the system and records images of the ring. Movies are analyzed using the open source software IMAGEJ [28] and we focus on the final snapshot for the present study. We observe that when the ring is composed of a small number of beads, it has a circular shape. Under the action of gravity and above some number of beads N_f, the

Published in : Physical Review E (2025), vol. 112, n°4, L043403
DOI: 10.1103/pznx-lrxq
Status : Postprint (Author's version)

shape becomes flat at the bottom. Further increasing the number N of beads allows the system to deform more and more. The flattened ring adopts a capsule-like shape. Adding more and more magnetized beads from the initial state, and buckling appears in the top part of the ring. Just after buckling, adding a few beads leads to the collapse of the ring into a zipped state when a critical number N_z of particles is reached. There, two opposite parts of the ring are in contact due to magnetic forces. Only the edges of the ring are still rounded. Once zipped, the chains remain attached. The transition is irreversible without external manipulation. The three states (circular, capsule-like, and zipped) are represented in Fig. 2 from left to right. We show pictures, numerical simulations, and sketches of the three cases at different numbers N of beads.

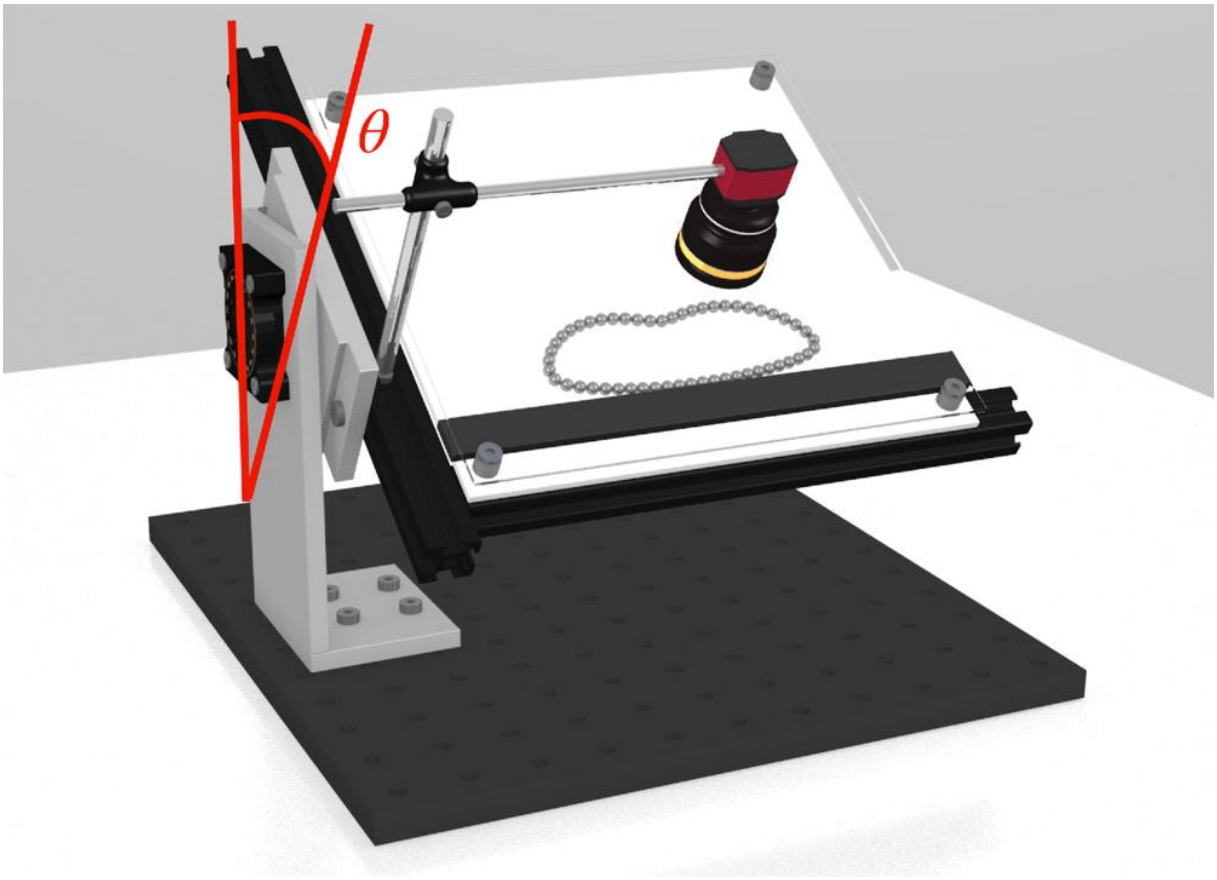

Fig. 1. Sketch of the experimental setup composed of a 2D cell containing the ring. The cell is itself tilted by angle θ with the vertical axis to change the gravity conditions.

Image treatment of the magnetoring in the experimental setup allows to determine its general shape and more specifically the fraction x of particles participating to the curvature of the object. For a circular ring, $x = 1$ while a simple horizontal chain will gives $x = 0$. Figure 3 shows the experimental value of this fraction x of beads as a function of ring size N for three different cell tilting ($\vartheta = 30\circ$, $60\circ$, and $90\circ$ in blue, red, and green, respectively). Two different kinds of beads with different magnetization are used : $\mu_{\mathrm{Cr},5}$ (empty dots) and $\mu_{\mathrm{Ni},5}$ (full dots). However, their diameter and mass are identical. The error bar account for the standard deviation is over three measurements.

Published in : Physical Review E (2025), vol. 112, n°4, L043403
DOI: 10.1103/pznx-lrxq
Status : Postprint (Author's version)

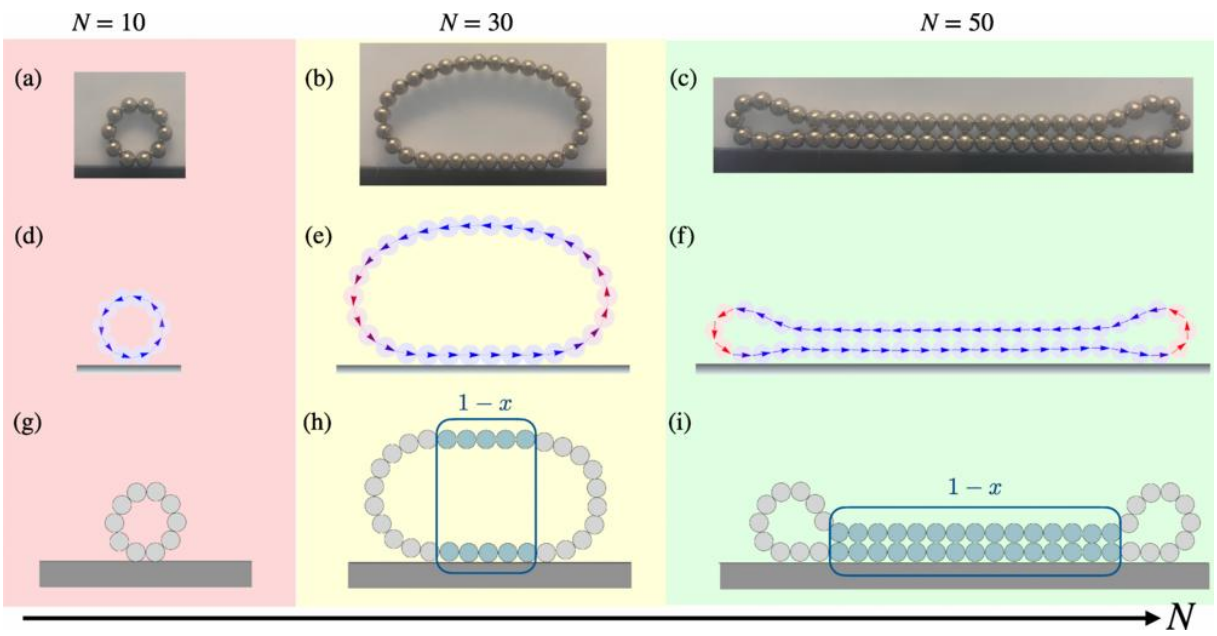

Fig. 2. From left to right, the system is made of 10, 30 and 50 beads. (a)–(c) Pictures of the system under gravity. (d)–(f) Numerical simulation of the same system. Color of a bead account for the angle difference with its neighbors. Arrows represent the dipoles. (g)–(i) Sketch of the system on which we base our analytical model. In addition, a color is assigned to each shape and is reported in other figures of this Letter.

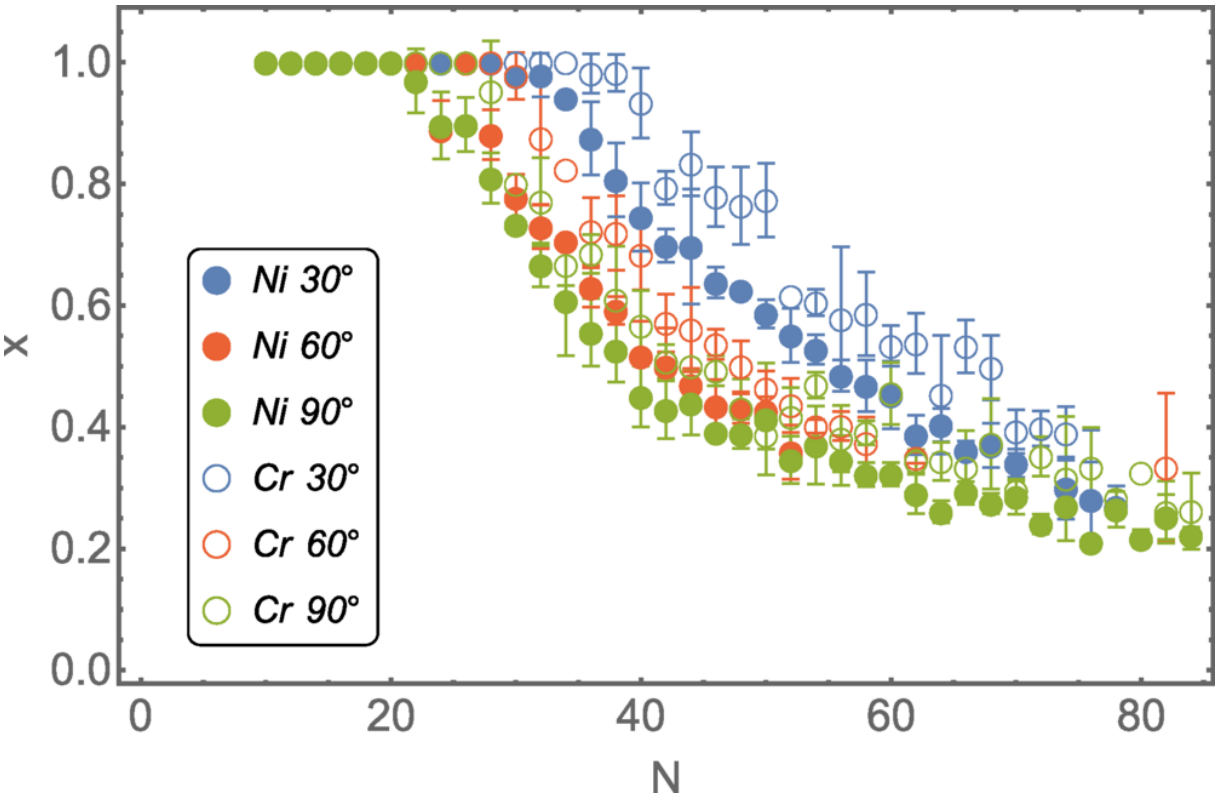

Fig. 3. Proportion x of beads in the curved part of the system as a function of the total number of beads. In blue, θ=30∘, in orange θ=60∘, and in green, θ=90∘ meaning the system is vertical.

The plateau is where x = 1 corresponds to the circular state. Then, x decreases with N as the ring deforms and flattens. In addition, Fig. 3 also shows the behavior of the ring when the cell is not

Published in : Physical Review E (2025), vol. 112, n°4, L043403
DOI: 10.1103/pznx-lrxq
Status : Postprint (Author's version)

completely vertical. Reducing the gravity effect on the ring delays the first appearance of the capsule-like shape, i.e., the plateau is longer for small ϑ values. In addition, increasing the magnetic moment also delays the capsule-like shape.

Nonetheless, the transition between capsule-like and zipping is difficult to discern in Fig. 3. To obtain a clear view on the transition between these states, Fig. 4 represents only the nickel beads in the vertical cell (green full dots). The background colors remind us of those of Fig. 2. To highlight the transition from capsule-like to zipped state, we plot in the bottom of Fig. 4 the number of beads that forms the curved part *Nx* as a function of the total number of beads *N*. In this situation, we evidence a plateau in the green part, meaning the number of beads in the curved part is constant.

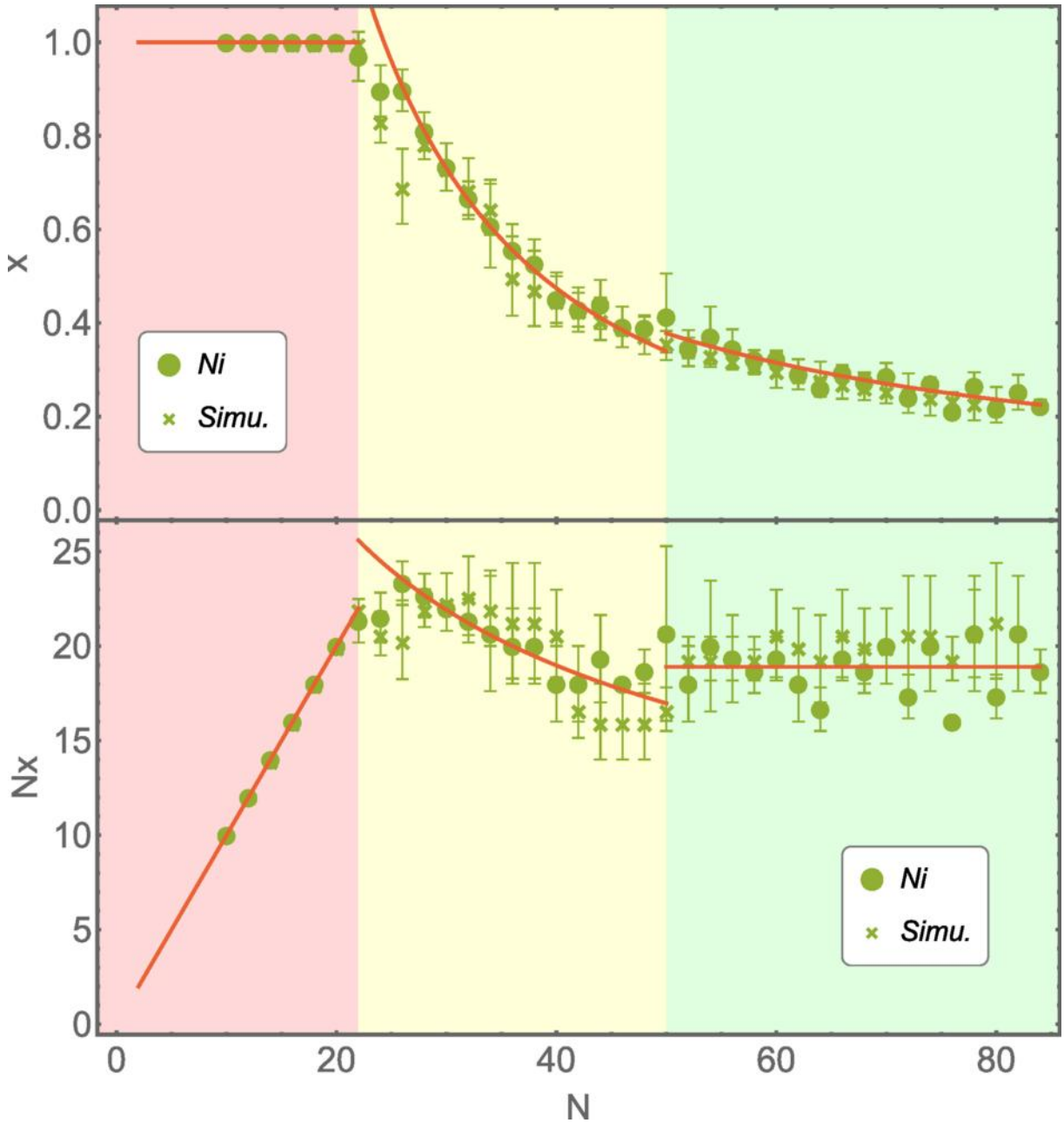

Fig. 4. Top: Fraction of particles *x* participating to a (concave) curvature on the object, as a function of *N* for $\mu_{Ni} \simeq 6.25\ 10^{-2}$ Am^2, and simulation at $\vartheta = 90^\circ$ meaning the system is vertical. Bottom: Number of beads *Nx*

Published in : Physical Review E (2025), vol. 112, n°4, L043403
DOI: 10.1103/pznx-lrxq
Status : Postprint (Author's version)

participating to a (concave) curvature on the object in the same conditions. In both figures, the error bar correspond to the standard deviation over three experiment or simulations. In the red region, the shape is a ring, in yellow, the shape is a flattened ring and in the green region, the shape is a zipped ring.

To explain those experimental observations, let us consider the magnetic interaction between beads. Spheres which are uniformly magnetized can be seen as point-like dipoles $\vec{\mu}$ [29]. The short-range interaction between two dipoles $\vec{\mu}_1$ and $\vec{\mu}_2$ separated by a distance $\vec{r}_{12}$ is given by

$$U_{12} = \frac{\mu_0}{4\pi}\left[\frac{\vec{\mu}_1.\vec{\mu}_2}{r_{12}^3} - \frac{3(\vec{\mu}_1.\vec{r}_{12})(\vec{\mu}_2.\vec{r}_{12})}{r_{12}^5}\right]. \quad (1)$$

In our problem, all dipoles within the system have similar moments $|\vec{\mu}_i|=\mu$, and many beads are in contact, i.e., they are at a distance $r_{12}=d$. We consider, therefore, a nondimensional characteristic energy

$$U_0 = \frac{\mu_0 \mu^2}{4\pi d^3} \quad (2)$$

for defining a dimensionless potential $u = \sum_{i,j} U_{ij}/U_0$. For two dipoles in contact, the ground state is therefore $u_{12} = -2$ when both dipoles are parallel to the vector that joins their centers. Therefore, the natural way to assemble dipoles is to form a chain made of aligned dipoles. In a previous work, we rigorously calculated the energy of a chain of N dipoles as well as a ring [18,30]. These cases are described in full detail in the *Appendix: Circular ring*.

Considering the short-range nature of dipolar interactions, only nearest neighbors are considered in our model. Based on the calculations in the *Appendix: Circular ring*, the dimensionless energy of a capsule-like shape is given by

$$u_f = -2N + 4\frac{\pi^2}{xN} + \frac{\mathrm{Bo}xN^2}{2\pi}, \quad (3)$$

where the Bond number is given by

$$\mathrm{Bo} = \frac{m\,g\,d}{U_0}. \quad (4)$$

The circular chain is slightly deformed by gravity with a fraction x of grains contributing to the curvature of the object. The derivative of u_f allows one to determine the minimum value of this potential

$$x = \sqrt{\frac{8\pi^3}{\mathrm{Bo}N^3}} \quad (5)$$

providing a scaling $x \propto N^{-3/2}$, which is fitted on the data of Fig. 4 in the capsule-like shape. Also, we know that when N is below the first critical number N_f, the shape is a ring and x=1. This condition leads to the scaling

$$N_f \propto \frac{1}{\sqrt[3]{\mathrm{Bo}}}, \quad (6)$$

explaining a circular shape when gravity effects are lower than magnetic effects.

Published in : Physical Review E (2025), vol. 112, n°4, L043403
DOI: 10.1103/pznx-lrxq
Status : Postprint (Author's version)

When the number of beads N becomes larger, the system tends to be zipped. We consider the zipping state as two chains in contact and opposite directions. Their extremities are connected and form small rings. Experimental and numerical observations lead us to the conclusion that the number of beads that make up the curved part is constant and therefore Nx=const. as observed in Fig. 4(b). In a first approximation, we consider an additional adhesion term in Eq. (3) being $-\mathrm{Bo}N\frac{(1-x)}{2}$. After minimizing energy, we find the scaling

$$N_z \propto \frac{1}{\mathrm{Bo}} + b, \quad (7)$$

with $b \simeq Nx$ being a constant linked to the number of beads in the remaining curved parts at both extremities of the zipped magnetostructure. It corresponds to the final plateau in Fig. 4 (bottom). One should remark that this characteristic number of beads b is in the range 18 to 24 in our experiments. More details about the calculations behind Eq. (7) are made in the *Appendix: Circular ring*.

The experimental data are located in a narrow window of the Bond number, i.e., Bo ∈ [1.8 10^{-3},8 10^{-3}]. To validate the above scaling laws derived from nearest-neighbor models, data are completed with the help of numerical simulations based on the *discrete element method* (DEM) that we described elsewhere [25,31]. The algorithm allows us to change a plethora of parameters such as mass, size, and magnetization of particles, and gravitational force, thus extending the range of Bo. The DEM model allows us to also consider all interaction pairs in the system described by Eq. (1). Another benefit of the numerical simulation is in the visualization of the dipole orientations as represented in Figs. 2(d)–2(f). Our simulations are constrained in two dimensionss. At the beginning of the simulation, the beads are placed to form a ring shape, with dipoles oriented head to tail. The ring is also subject to gravity and eventually flattens and collapses. We can also increase gravity gradually to avoid inertial effects. The results of the simulations are drawn in Figs. 2(d)–2(f), confirming that the numerical model captures all shapes. From the numerical data, x is extracted and plotted in Fig. 4 for the same parameters as the nickel beads. The agreement is excellent since experimental and numerical data superimpose. Since numerical simulations reproduce experimental data, more simulations are performed extending the range to Bo ∈ [0, 15 10^{-3}].

The data about transitions are illustrated in a phase diagram represented in Fig. 5. There, we plot the critical numbers of beads N_f and N_z needed to reach different states for any specific value of the Bond number. The three colors associated to the shapes, already used in Figs. 2 and 4, are also represented. The open triangle represents 3mm chromium beads which are not plotted in Figs. 3 and 4. The crosses are numerical simulations over the Bo range. The curves are fits of the scaling laws $N_f \propto \mathrm{Bo}^{-1/3}$ and $N_z \propto \mathrm{Bo}^{-1} + b$. The latter transition is fitted with a value $b = 24$ consistent with experimental observations. This phase diagram shows that the higher the Bond number, which means either a higher gravity component or lower magnetic interaction, the lower N_f and N_z, and conversely. When Bo ≃ 0, the curves diverge meaning the shape will remain a ring in the absence of gravity, which occurs when the plate is horizontal. In this diagram, one observes that all numerical and experimental data collapse on scaling laws. Although the scaling laws are derived from a nearest-neighbor model, the data show an agreement with a detailed numerical model. Scaling laws are therefore robust.

Published in : Physical Review E (2025), vol. 112, n°4, L043403
DOI: 10.1103/pznx-lrxq
Status : Postprint (Author's version)

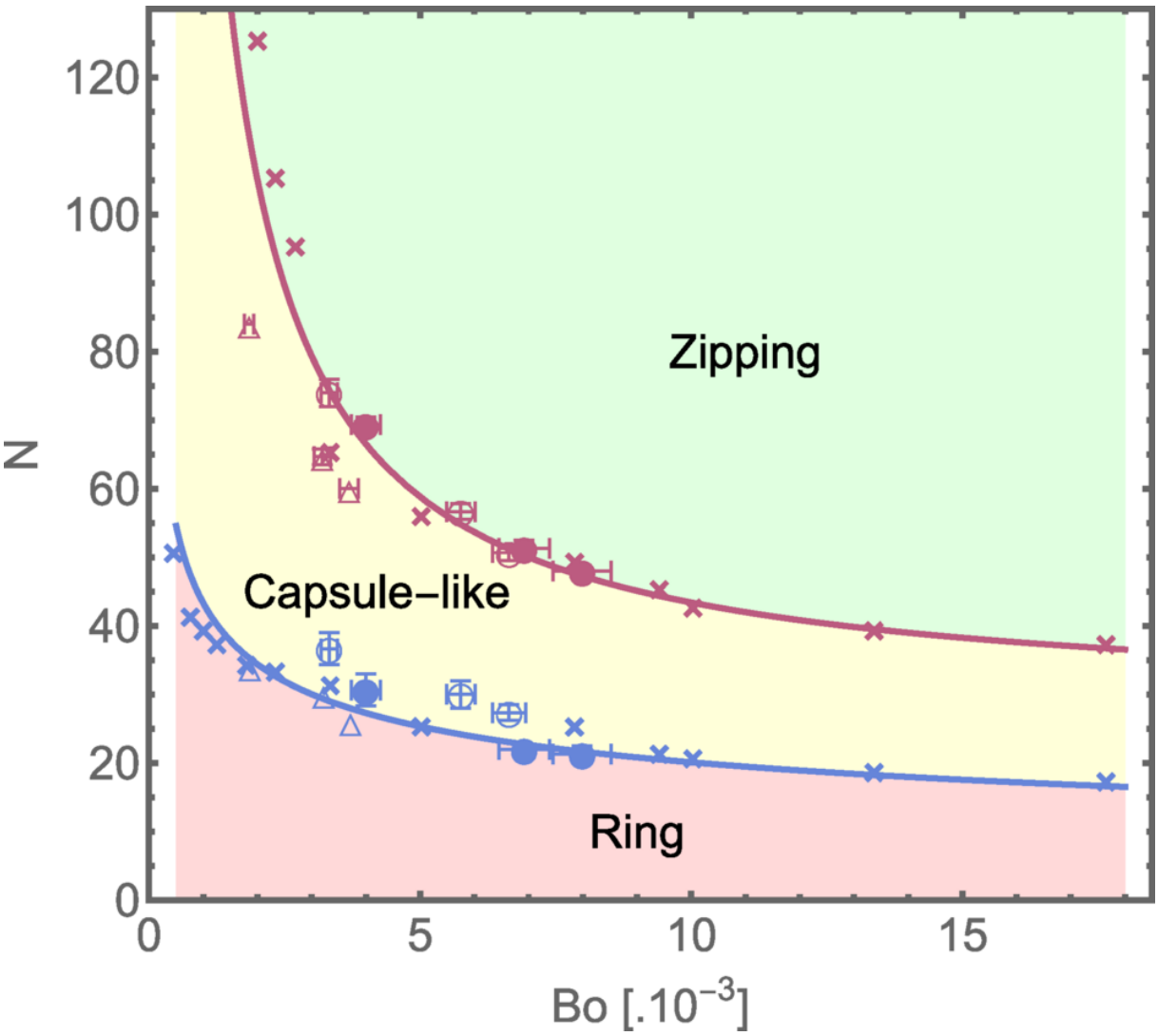

Fig. 5. Phase diagram representing the shapes and the transitions for a specific value of the Bo and the total number of beads composing the system. Circles and open triangles are experimental data and crosses are numerical data at which the transition occurs, and curves are fits to guide the eyes following Eqs. (6) and (7). Larger Bond number means either larger gravity component and/or lower magnetic interaction and conversely.

In conclusion, we show that a ring made of *N* permanent magnetic beads can experience different shapes depending on gravity's condition and the beads' magnetization. The model proposed above can predict this shape depending on the competition between the two latter effects (defined as a Bond number) and *N*. Although our model neglects friction and only considers nearest-neighbor interactions, it nonetheless shows good agreement with both experimental and numerical data.

Beyond its immediate application in controlling the shape of magnetically responsive rings, this macroscopic system serves as a minimal yet powerful platform to study adhesionlike phenomena. It captures the essential features of biological adhesion, where the shape changes arise from the interplay between mechanical instability and attractive forces, as in morphogenetic processes or tissue zipping. By tuning magnetization or geometry, the model offers design guidelines to either suppress or promote zipping, enabling the creation of soft, flattened objects with predetermined aspect ratios. Furthermore, when embedded in an elastic matrix or actuated by external fields, such

Published in : Physical Review E (2025), vol. 112, n°4, L043403
DOI: 10.1103/pznx-lrxq
Status : Postprint (Author's version)

assemblies could inform the development of reconfigurable magnetoresponsive materials. These systems hold promise for diverse applications, including soft actuators, shape-morphing surfaces, and magnetically driven soft robots. Thus, our work bridges soft matter physics, bioinspired engineering, and functional material design.

Acknowledgment

This work is financially supported by the University of Liège through the CESAM Research Unit.

Data availability

The data that support the findings of this article are openly available [32].

Appendix: Circular ring

An approximate way to calculate the total energy u of the chain is to consider the short-range character of the dipolar interaction, restricting the calculation to nearest neighbors. When a local curvature is induced in the chain such that two successive dipoles have a slight deviation angle α, their interaction potential (2) becomes $u_{12} = -2\cos\alpha$ and for small angles

$$u_{12} = -2 + \alpha^2 + \mathcal{O}(\alpha)^4. \quad \text{(A1)}$$

The quadratic behavior for any small angular deviation α provides the elastic character to the dipolar chain. A ring of N beads can be treated similarly using a constant angle $\alpha = 2\pi/N$ between successive dipoles. Therefore, the ring energy is given by

$$u_\circ = -2N + \frac{4\pi^2}{N}. \quad \text{(A2)}$$

When the ring is placed vertically, one should also consider the gravity potential $U_g = NmgR$ where the radius of the circle is $R = Nd/2\pi$ and m is the mass of each bead. Taking into account Eq. (2), one has

$$u_\circ = -2N + \frac{4\pi^2}{N} + \mathrm{Bo}\,\frac{N^2}{2\pi}, \quad \text{(A3)}$$

where Bo is the Bond number which compares both effects. In addition, when the ring flattens, only a fraction x of beads contributes to the curvature and we find $u_f = -2N + 4\frac{\pi 2}{xN} + \frac{BoxN^2}{2\pi}$ which is Eq. (3). The energy u_f/N is plotted on the top of Fig. 6 as a function of N for two different values of x and for $\mathrm{Bo} \approx 7.85 \times 10^{-3}$ which correspond to $g = 9.81$ and beads $\mu_{\mathrm{Ni},5}$. It appears that for $N < N_f$, energy is lower for $x = 1$ than for $x = 0.5$ suggesting it is more favorable to keep a ring shape, even with gravity. However, as the number of beads increases, x must decrease to minimize u_f/N.

Published in : Physical Review E (2025), vol. 112, n°4, L043403
DOI: 10.1103/pznx-lrxq
Status : Postprint (Author's version)

Zipping state

Concerning the second transition, we must add a term which takes the zipped state into account. Since dipoles from neighbor chains are antiparallel, we can approximate this term to $N(1-x)/2$, where $1-x$ is the proportion of beads in those chains. The dimensionless energy of this zipping state becomes

$$u_z = -2N + \frac{4\pi^2}{xN} + \frac{\mathrm{Bo}xN^2}{2\pi} - \mathrm{Bo}N\frac{(1-x)}{2}. \quad \text{(A4)}$$

Calling $c = Nx$ a constant, Eq. (A4) becomes

$$u_z = -2N + \frac{4\pi^2}{c} + \frac{\mathrm{Bo}cN}{2\pi} - \mathrm{Bo}\frac{(N-c)}{2}. \quad \text{(A5)}$$

Published in : Physical Review E (2025), vol. 112, n°4, L043403
DOI: 10.1103/pznx-lrxq
Status : Postprint (Author's version)

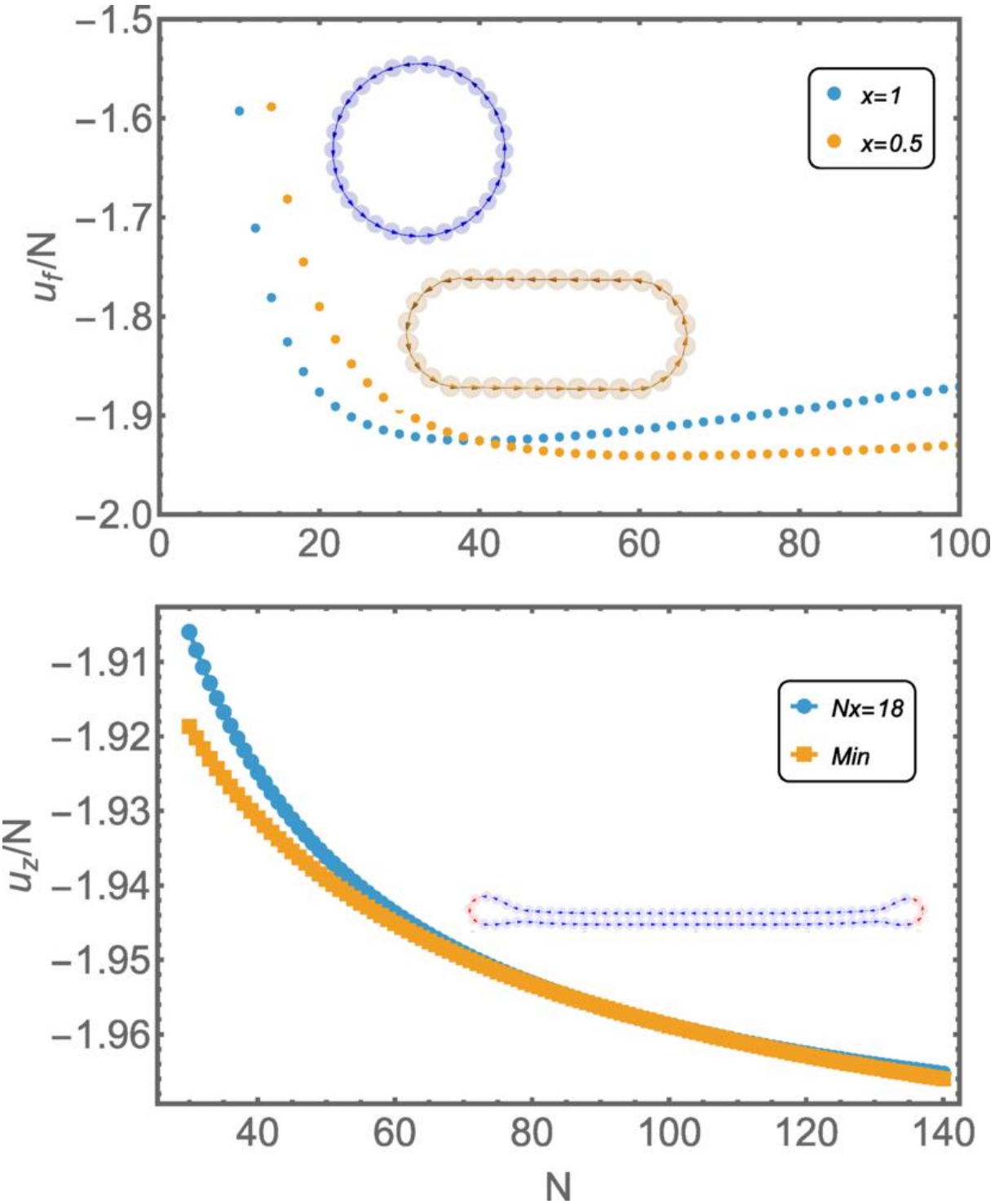

Fig. 6. Top: Energy u_f/N for capsule-like shape as a function of the number of beads. For $N < N_f$, one can see $u_f > u_o$, with u_o corresponding to the case $x = 1$. Bottom: Energy u_z/N for zipped states as a function of N for $Nx = 18$ which correspond to our observations and for the minimization of Eq. (A4). When N is small, the energy is larger than the minimum of u_z. Nonetheless, when $N > N_z$, both lines converge.

Looking for the minimum, one finds

$$\frac{\partial u_z}{\partial c} = 0 = \frac{-4\pi^2}{c^2} + \frac{\mathrm{Bo}N}{2\pi} + \frac{\mathrm{Bo}}{2}, \quad \text{(A6)}$$

Published in : Physical Review E (2025), vol. 112, n°4, L043403
DOI: 10.1103/pznx-lrxq
Status : Postprint (Author's version)

and

$$\frac{4\pi^2}{c^2} = \frac{\mathrm{Bo}N}{2\pi} + \frac{\mathrm{Bo}}{2}. \quad \text{(A7)}$$

Finally, we obtain a scaling for N depending on Bo by isolating the former. It appears that

$$N_z \propto \frac{1}{\mathrm{Bo}} + b, \quad \text{(A8)}$$

where b is a constant. The energy u_z/N is presented in the lower part of Fig. 6 as a function of N for Bo ≈ 7.85×10^{-3}. The plot includes the case where $Nx = 18$ is held constant as well as configurations where the parameters N and x are chosen to minimize u_z/N. One can observe that when N is small, both curves diverge and it is not favorable to zip. However, when N becomes large enough, both curves superimpose, which means the zipped state with small rings at the extremities is close to the energy minimum of the function u_z given by Eq. (A4).

References

[1] A. L. Hazel and T. Mullin, Phil. Trans. R. Soc. A. **375**, 20160227 (2017).

[2] E. Sackmann and A.-S. Smith, Soft Matter **10**, 1644 (2014).

[3] M. K. Chaudhury, A. Chakrabarti, and A. Ghatak, Eur. Phys. J. E **38**, 82 (2015).

[4] E. Trubuil, A. D'Angelo, and J. Solon, Cells Development **168**, 203777 (2021).

[5] A. Goriely, *The Mathematics and Mechanics of Biological Growth*, 1st ed. (Springer, New York, 2017).

[6] J. Bico, B. Roman, L. Moulin, and A. Boudaoud, Nature (London) **432**, 690 (2004).

[7] R. Dufour, P. Brunet, M. Harnois, R. Boukherroub, V. Thomy, and V. Senez, Small **8**, 1229 (2012).

[8] L. J. Gibson, J. Biomech. **38**, 377 (2005).

[9] L. Rossi, Frontiers of Nanoscience **13**, 1 (2019).

[10] M.Klokkenburg, R. P. A. Dullens, W. K. Kegel, B. H. Erné, and A. P. Philipse, Phys. Rev. Lett. **96**, 037203 (2006).

[11] H. Schmidle, C. K. Hall, O. D. Velev, and S. H. L. Klapp, Soft Matter **8**, 1521 (2012).

[12] M. Hubert, O. Trosman, Y. Collard, A. Sukhov, J. Harting, N. Vandewalle, and A.-S. Smith, Phys. Rev. Lett. **126**, 224501 (2021).

[13] Y. Collard, G. Grosjean, and N. Vandewalle, Commun. Phys. **3**, 112 (2020).

[14] Z. Ren, W. Hu, X. Dong, and M. Sitti, Nat. Commun. **10**, 1 (2019).

[15] X.Wang, B. Sprinkle, H. K. Bisoyi, T. Yang, L. Chen, S. Huang, and Q. Li, Proc. Natl. Acad. Sci. USA **120**, e2304685120 (2023).

Published in : Physical Review E (2025), vol. 112, n°4, L043403
DOI: 10.1103/pznx-lrxq
Status : Postprint (Author's version)

[16] H. Gu, Q. Boehler, H. Cui *et al.*, Nat. Commun. **11**, 2637 (2020).

[17] H. Gu, M. Möckli, C. Ehmke *et al.*, Nat. Commun. **14**, 1263 (2023).

[18] N. Vandewalle and S. Dorbolo, New J. Phys. **16**, 013050 (2014).

[19] S. Egri and G. Bihari, J. Phys. Commun. **2**, 105003 (2018).

[20] D. Vella, E. du Pontavice, C. L. Hall, and A. Goriely, Proc. R. Soc. A. **470**, 20130609 (2014).

[21] C. L. Hall, D. Vella, and A. Goriely, SIAM J. Appl. Math. **73**, 2029 (2013).

[22] I. Stanković, M. Dašić, J. A. Otálora, and C. García, Nanoscale **11**, 2521 (2019).

[23] A. Wafflard, N. Vandewalle, and E. Opsomer, New J. Phys. **25**, 063024 (2023).

[24] D. S. Borges, H. J. Herrmann, H. A. Carmona, J. S. Andrade, Jr., and A. D. Araujo, Phys. Rev. Lett. **126**, 118001 (2021).

[25] A.Wafflard, E. Opsomer, and N. Vandewalle, Phys. Rev. E **110**, 054608 (2024).

[26] N. Vandewalle and A. Wafflard, Phys. Rev. E **103**, 032117 (2021).

[27] S. Hidalgo-Caballero, Y. Y. Escobar-Ortega, R. I. Becerra- Deana, J. M. Salazar, and F. Pacheco-Vázquez, J. Magn. Magn. Mater. **479**, 149 (2019).

[28] J. Schindelin, I. Arganda-Carreras, E. Frise *et al.*, Nat. Methods **9**, 676 (2012).

[29] J. D. Jackson, *Classical Electrodynamics*, 3rd ed. (Wiley, New York, 1998).

[30] R. Messina, L. Abou Khalil, and I. Stankovic, Phys. Rev. E **89**, 011202(R) (2014).

[31] S. Luding, Eur. J. Environ. Civ. Eng. **12**, 785 (2008).

[32] A. Wafflard, S. Van der Heyde, J. Dhyon, E. Opsomer, and N. Vandewalle, Magnetic ring data (2025), https://github.com/GRASP-LAB/Magnetic-Ring/tree/main.